Dusk Scene Simulation based on the Piecewise Multiple Regression of a Time-Series Color Block's Images

Chen-Chung Liu
Chin-Yi University of Technology
Associate Professor
ccl@ncut.edu.tw

Chi-Chao Yang
Chin-Yi University of Technology
Student
guitar3931@yahoo.com.tw

Guan-Nan Hu
Chin-Yi University of Technology
Student
robert6pill@yahoo.com.tw

摘要

本文介紹一個針對西邊風景影像在任何時間的模擬影像之高效率、新穎的演算法。此演算法結合了離散餘弦變換、表格查尋及統計的分段多元迴歸。首先，我們使用在同一天的固定時間間距的顏色方塊之逆光影像，將它們作離散餘弦轉換(Discrete Cosine Transform)後作為西邊風景影像之時間模擬的參考數據庫。然後，我們從這個參考數據庫建立光的三原色(紅色、綠色、藍色)的 DCT 係數隨時間變化之分段多元迴歸最佳貼合函數(best fitting functions)。最後，使用輸入西邊風景影像和原始時間之時間模擬黃昏景色演算法(ADSS)於焉完成。

為展示我們提出的演算法的效率，我們輸入且模擬各種各樣的西邊風景影像。實驗結果證明，我們提出的演算法可以從輸入的西邊風景影像精確地模擬出該西邊風景影像在任何時間的模擬黃昏景色的影像。

關鍵詞: 黃昏、離散餘弦變換、表格查尋、分段多元迴歸、模擬

Abstract

Sunrise and Sunset are the most beautiful scenes of a day, but they appear only in a very short time interval and people are almost always too busy to wait for their coming. In this paper, we propose an efficient strategy for simulating the dusk scenes from an outdoor scene image taken due west before the Sunset time. It is a hybrid approach combining the piecewise multiple regression of data, the discrete cosine transformation, and a look-up table algorithm. First, several color-block images taken due west at afternoon of a day were used to construct the reference database. We find the best fitting functions for these color-block images on each plane (red, green, and blue) individually. Then we establish the databases of the DCT coefficients with respect time. Finally, the algorithm of dusk scene simulation (ADSS) is able to synthesize the dusk scene from a outdoor scene taken in afternoon.

To explore the utility and demonstrate the efficiency of the proposed algorithm, simulations under various input images are conducted. The experiment results show that our proposed algorithm can precisely simulate the desired Sunset scenes at an assigned Sunset time and has three advantages: (A) Using the color-block images instead of using the scene images of a place to create the reference database, the database can be used for any outdoor scene taken at anywhere at afternoon. (B) Taking the piecewise multiple regression on the DCT coefficients of scene images instead of taking the piecewise multiple regression on the spatial pixels of scene images, it simplifies the regression procedure and save the processing time. (C) Using look-up table algorithm to save much time.

Keywords: Dusk, DCT, Look-up Table, multiple regression, Simulation.

1. Introduction

Sunrise and Sunset are the most beautiful scenes of a day, but they appear only in a very short time interval and people are almost always too busy to wait for their coming. If one can construct the Sunset (or Sunrise) scene of a scene image taken at anytime, then people shall no longer regret of missing the beautiful moments of their life.

The most special difference between a noon scene and a dusk (or dawn) scene is the colors of the sun and the sky. The Earth's atmosphere contains both air molecules and tiny aerosols (much tinier than the wavelength of the visible light-ray from the Sun), both of which scatter the visible light-ray from the Sun which grazes the Earth's atmosphere.

The scattering from both air molecules and aerosols is predominantly the Rayleigh scattering [1-4].The intensity of light scattered by a single tiny particle from a beam of light is a function of the original intensity of entrance light, the scattering angle between the direction of incidence and the direction of observation, the large distance from the particle to the observer, the wavelength of entrance light, the refractive index of particle, and the diameter of the particle, and the concentration of particles. It is a very complicated function.

According to the Rayleigh scattering law of light, the scattered light is polarized at a large angle with respect to the direction of the sun's light and blue light is scattered more strongly than red light. Sunlight goes through very little atmosphere when the sun high in the sky, so little scattering takes place. Due to the spectral sensitivity of the human visual system, the sky far away to the sun appears light blue (and not violet) and the sky close to the sun appears mostly white (the sun's color).When the Sun is low in the sky at Sunrise or at Sunset, the Sun's light has to travel through a much thicker layer of atmosphere to reach us on the ground owing to the oblique angle. This extra distance causes multiple scatterings and Mie scattering of blue light, the sky appears less bright and redder than that at noon because more blue light than red light is scattered out of the solar light-rays, leaving an excess of red light.

It is very difficult to obtain the concentration and the diameters of the air molecules and the tiny aerosols in the Earth's atmosphere, so it is difficult to estimate the colors of an outdoor scene precisely by using the Rayleigh scattering law of light without suitable instruments. In 2002, Thompson derived a spatial post- processing algorithm of night scene [5] based on the visual noise (VN) and the loss of acuity (LA). There are four strategies in Thompson algorithm: (A) color space transform (CST), (B) day to night conversion (DNC), (C) night filter (NF), and (D) Gaussian noise generator (GNG). It can generate more realistic night scene, but it neglects the time factor so it cannot clearly illustrate the differences between early night, middle night and midnight. Alexander Toet used the method introduced by Welsh et al to transfer a source image's color characteristics to a grayscale target image (night vision imagery)[6,7]. They search a color source image that resembles the target scenes first. Secondly, they transformed both the source image and the target image into a perceptually miscorrelated color space. Third, they searched for the best matching source pixel for each target pixel from the source image by using the first order statistics of the luminance distribution in a 7×7 window around the source and target pixels. Finally, they assigned the matching pixel's chromaticity values of the source image to the target pixel. Although they effectively give single-band intensified night vision gray imagery a full color day-time image, but to find a suitable resembled color source image for the target image is not easy, and the final colors of the chromatic target image completely depends on the colors of the source image. They are not the true colors of the target image taken in day. Other papers about the scenes can be found in [8-19].

The multiple regression is a related statistical method, it is used to model the relationships between several independent variables and a dependent variable by fitting an equation to observed data. Numerous experiments have shown that the multiple regression models can be used to make accurate predictions. Multiple regression procedures are very widely used in the social and natural sciences today[20-22]. It might be a good and suitable method for us to simulate the time scene.

The red, green and blue are the primary components of color image in spatial domain. It is reasonable to take the multiple regression on each component individually. But, the spatial pixels of an image are often correlative, so the spatial domain of an image is not suitable for taking multiple regression. The DCT has properties of noise filtering, miscorrelation, and feature preservation. It is often used as a preprocessing step followed by a sophisticated algorithm in image processions, and it always has good performance while one combines the DCT block transformation with other techniques. In some cases, it has been showing that the processing based on DCT has significantly better results than the directive pixel based processing [23,24]. To take time scene simulation on the DCT domain by using multiple regressions will be a good idea. The outdoor scene's phenomena before sunset is quite different to that after sunset. To take regression on those data taken before sunset and that of being taken after sunset at one time should obtain a mistake result. Taking piecewise multiple regression on them can avoid the mistake. The remainder of this paper is organized as follows: Section 2 presents the algorithm of Sunset scenes simulation (ASSS). Empirical results are described in the Section 3. Finally, Section 4 concludes this paper.

2. The Algorithm of Sunset Scenes Simulation (ADSS)

2.1 The construction of the multiple regression functions database

The basic understanding of color perception of the human visual system shows the fact, which human eyes pick out the color of an object illuminated by white light is the reflection of selected wavelengths of light by that object [25-26]. The appearance color of an object can be considered as the object absorbing all colors except the colors that are reflected. For example, a red object illuminated by white light absorbs nearly all of the wavelengths except those corresponding to red light. Although there are an unlimited number of colors just as there are immeasurable quantities of real numbers on a number line, colors of the range of human visual sensations can be produced by the mixtures of finite visual lights of various wavelengths. Human eyes have three cones shaped light detectors [27]. Each cone is sensitive to a special range of colors. One is sensitive to primarily red, a second to primarily green, and a third to primarily blue. The three sensitivity ranges overlap in fact. Each cone transmits a nerve pulse to the brain at a rate proportional to the light's intensity of that cone detects. By combining the signal rates transmitted from three cones, the brain attempts to conclude what color and brightness of the light must be. Thus, to combine various quantities of three colors (red, green and blue) of light can turn out all colors that can be perceived for human.

In televisions, computer monitors, and colored image projection systems, only the three colors are enough to adequately represent any of the unlimited visible colors [28]. For measuring or reproducing color, a number of three dimensional color models have been defined; Color models like as HIS, L*a*b*, YIQ, YUV, and YCbCr are suitable for image processing applications, they are the reducing redundancy models of the image in RGB color space, obtained by some color transform from RGB color space, They are suitable for image processing applications, but not suitable for the color representation of a color image. The image in RGB color space is not suitable for image processing applications, because the image in RGB color space is highly correlated, but it is the most suitable for the color representation of a color image. Most imaging devices (CCD cameras, CRT monitors, etc) mimic the retina and utilize three separate channels calibrated for the detection of red, green and blue phosphors to render colors at every pixel on the screen [29]. The RGB color model is the most popular and natural color model. Due to it can compose any color adequately; it is frequently used in color image representation. R, G and B component of a color are given by:

$$R,G,B = k\int_{400}^{700} I(\lambda)\Phi(\lambda)S_{R,G,B}(\lambda)d\lambda \quad (1)$$

where k is a constant that defines the total overall brightness response of the human eyes, $I[\lambda]$ is the illumination spectral intensity of a color, $\Phi[\lambda]$ is the object spectral reflectivity, $S_{R,G,B}[\lambda]$ is the spectral sensitivity of the R or G or B channel of the detector and λ is the wavelength. The normalized red, green, and blue coordinates are defined as follow:

$$r = R/(R+G+B) \quad (2)$$

$$g = G/(R+G+B) \quad (3)$$

$$b = B/(R+G+B) \quad (4)$$

where R, G and B are the intensities of red, green, and blue light at a given pixel [30]. We demonstrated that color images could be represented using three primary colors.

In order to obtain the more accuracy regression of a scene image, the original image is first spilt into its R, G, and B components. Its final simulation image is reconstructed by composing these regression color components.

2.2 The construction of the multiple regression functions database

2.2.1 Multiple linear regression

When performing experiment, we frequently tabulate data in the form of ordered pairs $(x_1, y_1), (x_2, y_2), ..., (x_n, y_n)$ with each x_i distinct. Given the data, it is then usually desirable to be able to predict y from x by finding a mathematical model, that is, a function $y = H(x)$ that fits the data as closely as possible. One way to determine how well the function $y = H(x)$ fits these order pairs $(x_1, y_1), (x_2, y_2), ..., (x_n, y_n)$ is to measure the sum of squares of the errors (SSE) between the predicted values of y and the observed values y_i for all of the n data points.

Multiple linear regression is one of the widely used statistical techniques [31, 32]. This technique is used to find a polynomial function of degree k, $y = \beta_0 + \beta_1 x + \beta_2 x^2 + ... + \beta_k x^k$ as the predicting function, that has the minimum of the sum of squares of the errors(SSE) between the predicted values of y and the observed values y_i for all of the n data points $(x_1, y_1), (x_2, y_2), ..., (x_n, y_n)$ .The values of β_0, β_1, β_2, ..., and β_k that minimize

$$SSE(\beta_0, \beta_1, ..., \beta_k) = \sum_{i=1}^{n} [y_i - (\beta_0 + \beta_1 x_i + \beta_2 x_i^2 + ... + \beta_k x_i^k)]^2 \quad (5)$$

are obtained by setting the $k+1$ first partial derivatives $\frac{\partial}{\partial \beta_0} SSE(\beta_0, \beta_1, ..., \beta_k)$, $\frac{\partial}{\partial \beta_1} SSE(\beta_0, \beta_1, ..., \beta_k)$, ..., $\frac{\partial}{\partial \beta_k} SSE(\beta_0, \beta_1, ..., \beta_k)$ equal to zero, and solving the resulting simultaneous linear system of the so-called normal equations:

$$n\beta_0 + \beta_1 \sum_{i=1}^{n} x_i + \beta_2 \sum_{i=1}^{n} x_i^2 + ... + \beta_k \sum_{i=1}^{n} x_i^k = \sum_{i=1}^{n} y_i \quad (6)$$

$$\beta_0 \sum_{i=1}^{n} x_i + \beta_1 \sum_{i=1}^{n} x_i^2 + \beta_2 \sum_{i=1}^{n} x_i^3 + ... + \beta_k \sum_{i=1}^{n} x_i^{k+1} = \sum_{i=1}^{n} x_i y_i \quad (7)$$

$$\beta_0 \sum_{i=1}^{n} x_i^k + \beta_1 \sum_{i=1}^{n} x_i^{k+1} + \beta_2 \sum_{i=1}^{n} x_i^{k+2} + ... + \beta_k \sum_{i=1}^{n} x_i^{2k} = \sum_{i=1}^{n} x_i^k y_i \quad (8)$$

, and the matrix form solution of the normal equations system be

$$\begin{bmatrix} \beta_0 \\ \beta_1 \\ \beta_2 \\ \vdots \\ \beta_k \end{bmatrix} = \mathrm{B} = \left[X^T X\right]^{-1} \left[X^T Y\right] \quad (9)$$

,where

$$X = \begin{bmatrix} 1 & x_1 & x_1^2 & ... & x_1^k \\ 1 & x_2 & x_2^2 & ... & x_2^k \\ 1 & x_3 & x_3^2 & ... & x_3^k \\ \vdots & \vdots & \vdots & \vdots & \vdots \\ 1 & x_n & x_n^2 & ... & x_n^k \end{bmatrix}, Y = \begin{bmatrix} y_1 \\ y_2 \\ \vdots \\ y_n \end{bmatrix} \quad (10)$$

This paper proposed a way to construct the sunset scene of a scene image taken at anytime by TSSA. Fig.1 is the flow chart of the construction of the multiple regression functions database. At the beginning of the process, the R, G, and B planes of the decomposed color input image were split into non- overlapping 8 × 8 blocks, and then transferred into the frequency domain from the spatial domain by block DCT respectively. In the DCT domain, most of the signal information tends to be concentrated in a few low-frequency components. And the DC coefficient carry information about average luminance within the DCT blocks, the DC coefficient becomes the most meaningful when considering how the luminance is changing between the images [23, 24]. We took the average of the DC components of all the 8 × 8 DCT blocks to serve as the average value of the reflective color at that time. Then, we used piecewise multiple regression to find piecewise multiple regression functions of the DCT coefficients of these color-block images that were regularly photographed toward the west by fixed time interval from 15:00 to 18:30 of a day. These piecewise multiple regression functions were then constructed into a table as the database. Fig.2 shows the image of a color- block taken at 17:45, its R, G, B component images, and the images of DCT coefficients of the R, G, B component images. Table 1-3 are the tables of the average magnitudes of the 8 × 8

DCT coefficients for the R, G, B component images of the color-block. There are 64 entries for each table, the upper left entry is the block's mean and it is also called the DC value of the image, another 63 entries are called the AC values of the image. Table 1~ Table 3 shows that the DC value is much larger than the AC values. And the AC values are lesser at the higher entry's numbers. Fig.3, Fig.4, and Fig.5 show parts of the curves of the best fitting functions for color-block s' DC components with respect to time, the small circles are the original data, the vertical dash line is the boundary between the before sunset and the after sunset. Table 4 is the table of the best fitting functions' coefficients of the color-block image in DCT domain.

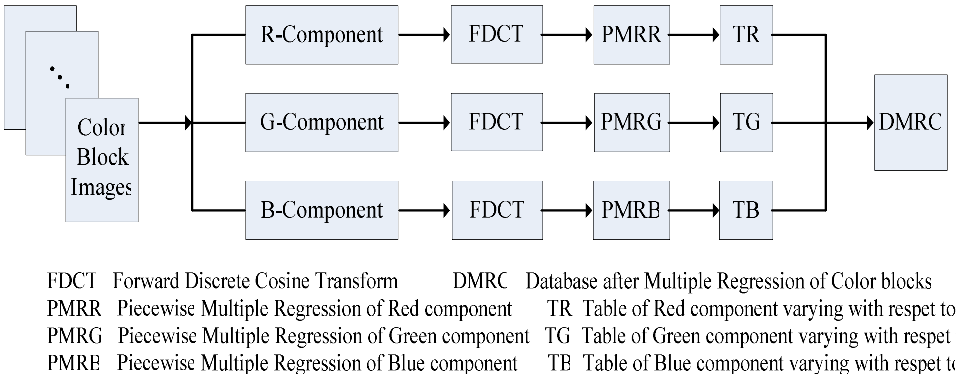

Fig. 1 The construction of the multiple regression functions database

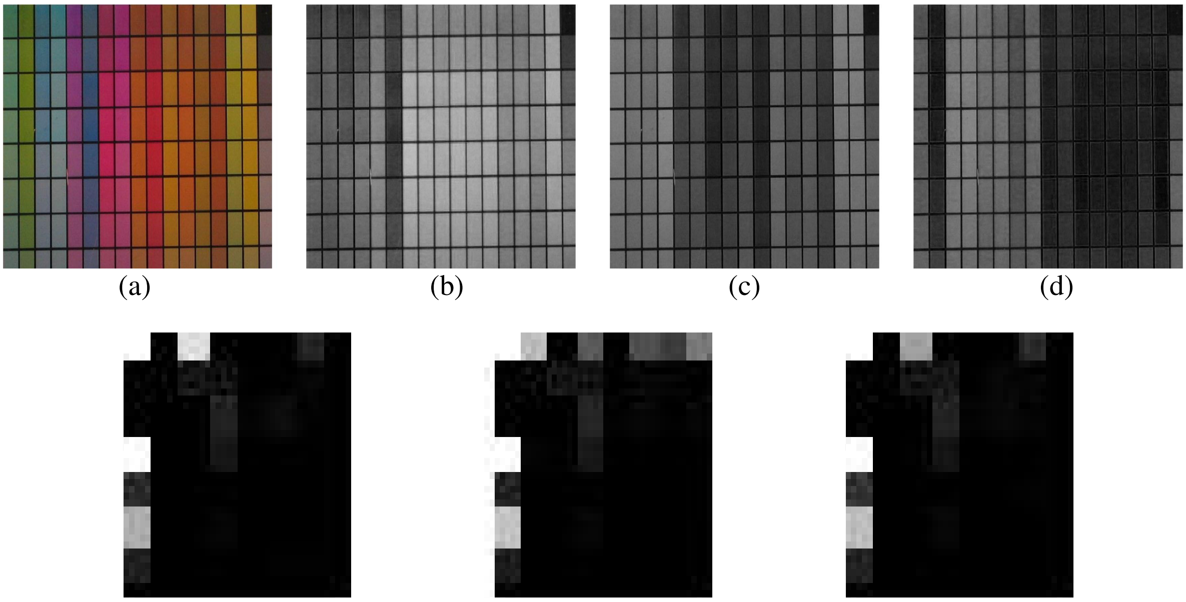

Fig. 2 The image of a color- block taken toward the Sun at 17:45(a) real image (b) R component image(c) G component image (d) B component image(e)The image of DCT coefficients of the R component(f)The image of DCT coefficients of the G component(g)The image of DCT coefficients of the B component.

Table 1 The DCT coefficients for the R component of the color-block image in Fig.2.

893.8228	-0.45261	0.868602	-0.1164	-0.09705	-0.27834	0.148148	-0.77643
-2.94184	-0.06269	0.078251	0.063731	-0.01928	0.00724	0.025912	-0.00203
-0.79647	-0.08613	-0.01123	0.130759	0.013335	0.043389	0.009456	-0.02649
1.55914	0.007455	-0.00411	0.089468	-0.03768	-0.01353	-0.00359	-0.00772
0.162109	-0.04689	-0.02009	0.00153	-0.01233	-0.00201	0.005597	-0.00795
0.676339	-0.05656	-0.0453	0.023209	0.002081	0.000104	0.002245	-0.00495
0.11855	-0.02559	-0.00031	-0.00632	0.002933	0.009982	0.004851	-0.00265
-0.30713	-0.00557	-0.00273	-0.00056	-0.00482	0.006392	-0.00146	0.00341

Table 2 The DCT coefficients for the G component of the color-block image in Fig.2.

589.9043	0.734307	-0.07695	0.350008	-0.08494	0.308407	0.232051	0.465971
-1.51106	0.019234	0.077048	0.070818	-0.01606	0.026507	0.017939	-0.01293
-0.28356	-0.06382	-0.01418	0.142056	0.008667	0.025829	0.007531	0.01963
1.003456	0.017033	0.00688	0.090062	-0.04392	-0.00146	-0.00364	-0.00399
0.127865	-0.05194	-0.02457	0.002267	-0.00855	0.001821	-0.00669	0.004322
0.765143	-0.06215	-0.02922	0.022936	-0.00021	-0.00744	-0.00799	-0.00333
0.11149	-0.00863	-0.00397	-0.0057	0.003457	0.005515	0.001468	-0.01019
-0.3085	-0.00547	-0.00186	0.004013	0.000163	-0.00435	-0.00367	-0.00394

Table 3 The DCT coefficients for the B component of the color-block image in Fig.2.

474.0879	-0.42085	0.626032	-0.15838	-0.06387	-0.15429	0.16869	-0.77979
-1.93456	-0.06226	0.077501	0.086982	-0.01613	0.023883	0.017536	-0.00817
-0.97552	-0.09372	-0.02877	0.134556	0.011908	0.035094	0.017732	-0.03484
1.007421	0.001975	0.008267	0.075614	-0.04308	0.001313	-0.00596	0.002432
0.197808	-0.03714	-0.0255	-0.01013	-0.00401	0.007147	0.012889	-0.00786
0.738631	-0.06534	-0.03933	0.028431	-0.0061	-0.00942	-0.00481	-0.01271
0.136035	-0.02628	-0.00045	0.005854	0.005896	-0.00524	0.00594	-0.00073
-0.31664	-0.00319	0.002837	-0.00113	-0.00488	0.001975	-0.00545	-0.00124

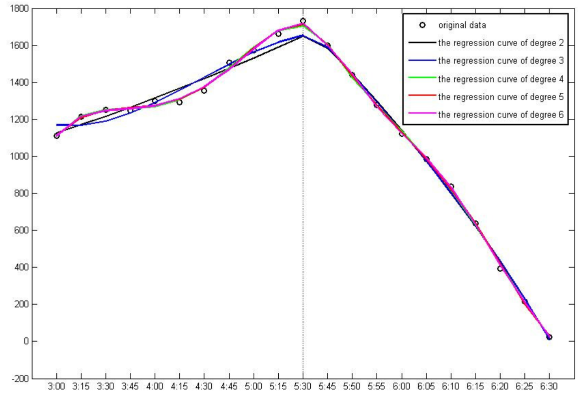

Fig. 3 Multiple regression curves of red component: the small circles are the original data.

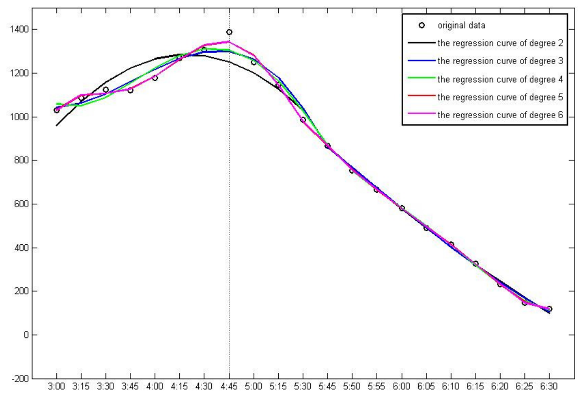

Fig. 4 Multiple regression curves of green component: small circles are the original data.

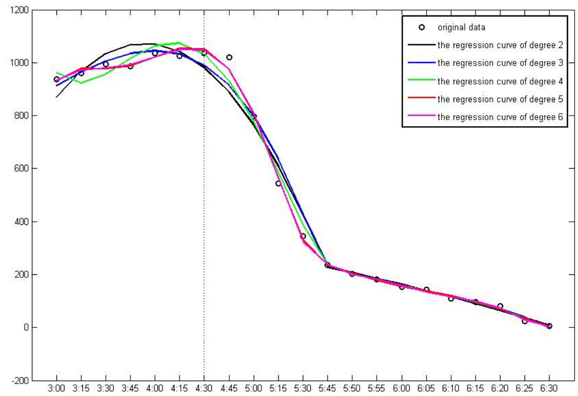

Fig. 5 Multiple regression curves of blue component: small circles are the original data.

Table 4 The table of the best fitting functions' coefficients of the color-block image's in DCT domain(a) R component (b) G component (c) B component.(α's are best fitting functions' coefficients before sunset, β's are best fitting functions' coefficients after sunset)

(a)

	α6	α5	α4	α3	α2	α1	α0
Order2					0.8951	41.6095	1083.808
Order3				-0.8539	17.5465	-48.4789	1200.368
Order4			-0.5487	13.4111	-105.117	340.7515	858.0081
Order5		-0.0218	0.1601	5.0266	-61.4074	245.2732	922.2726
Order6	-0.005	0.1722	-2.7656	26.4545	-139.63	374.969	850.3173

	β6	β5	β4	β3	β2	β1	β0
Order2					-4.5203	-124.315	1710.454
Order3				-0.2814	0.1225	-145.728	1734.597
Order4			0.358	-8.1563	57.7526	-303.226	1857.446
Order5		0.0707	-1.5858	11.3988	-29.7153	-136.607	1756.372
Order6	-0.0462	1.5969	-21.157	134.1868	-418.256	432.7963	1467.785

(b)

	α6	α5	α4	α3	α2	α1	α0
Order2					-11.5858	146.1621	823.8877
Order3				-1.6877	21.3235	-31.8859	1054.253
Order4			0.1398	-5.3219	52.5736	-131.047	1141.474
Order5		0.1287	-4.0428	44.1536	-205.349	432.3574	762.2576
Order6	-0.0025	0.2255	-5.5021	54.8418	-244.367	497.0496	726.3663

	β6	β5	β4	β3	β2	β1	β0
Order2					1.7727	-104.451	965.8083
Order3				0.2203	-1.8618	-87.6884	946.9088
Order4			0.2432	-5.13	37.2924	-194.694	1030.373
Order5		0.0374	-0.7857	5.2216	-9.0092	-106.493	976.8688
Order6	0.0136	-0.4124	4.983	-30.9709	105.5155	-274.328	1061.931

(c)

	α6	α5	α4	α3	α2	α1	α0
Order2					-15.8394	145.2647	740.2137
Order3				-0.8897	1.5106	51.3967	861.6637
Order4			0.4341	-12.1774	98.5718	-256.594	1132.567
Order5		0.1453	-4.2886	43.6878	-192.662	379.5747	704.3746
Order6	0.0071	-0.1303	-0.1312	13.2404	-81.5135	195.2863	806.6178

	β6	β5	β4	β3	β2	β1	β0
Order2					-0.4477	-19.5475	248.004
Order3				-0.3028	4.5484	-42.5901	273.9838
Order4			0.0353	-1.0799	10.2351	-58.1314	286.1059
Order5		0.0199	-0.5113	4.4194	-14.3623	-11.2753	257.6822
Order6	0.0222	-0.7136	8.894	-54.5888	172.3584	-284.913	396.368

2.3 The simulation image synthesis of dusk scene

Fig. 6 is the flowchart of the simulation scene dusk image of a scene. To synthesize the dusk scene image from a scene image photographed at afternoon, the input image photographed at time t_1 was divided into R, G, and B components firstly. The R, G, and B components are processed respectively with the same steps; they were transferred to the DCT domain by forward discrete cosine transform (FDCT) firstly. Then compared the DC component with the DC component of color-block at time t_1 to find the compensated coefficient c_1, to find the corresponding DC component $f_{i,j}(t_2)$ at time t_2 from looking up the database table, and then to combine $f_{i,j}(t_2)$ and c_1 to determine the final R, G, B components $g_{i,j}(t_2)$ of the simulation dusk scene at time t_2 on DCT domain. Finally, we took the inverse discrete cosine transform (IDCT) on $g_{i,j}(t_2)$, and combined them to form the color simulation dusk scene image at time t_2 of the scene.

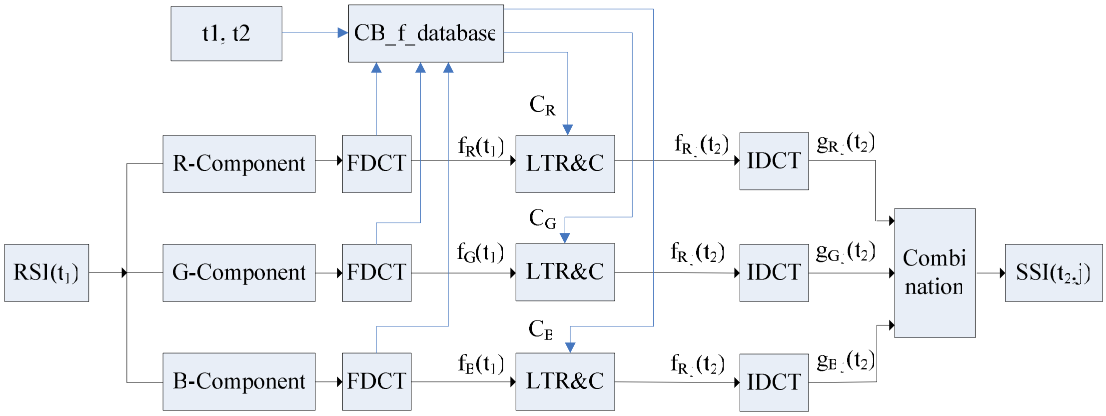

$RSI(t_1)$: Real Scene Image photographed at time t_1　　FDCT : Forward Discrete Cosine Transform
$f_R(t_1)$: R-component on frequency domain of image $f(t_1)$　　$f_G(t_1)$: G-component on frequency domain of image $f(t_1)$
$f_B(t_1)$: B-component on frequency domain of image $f(t_1)$　　LTR&C : Look_up Table Regression and Compensation
$f_{R\_}(t_2)$: The j-th degree simulation of R component at time t_2 on frequency domain　t_2 :The assigned time of simulation
$f_{G\_}(t_2)$: The j-th degree simulation of G component at time t_2 on frequency domain
$f_{B\_}(t_2)$: The j-th degree simulation of B component at time t_2 on frequency domain
IDCT : Inverse Discrete Cosine Transform　　CB_f_database : database of Color Blocks on frequency domain
$g_{R\_}(t_2)$: The j-th degree simulation result of R component at time t_2 on R.G.B domain
$g_{G\_}(t_2)$: The j-th degree simulation result of G component at time t_2 on R.G.B domain
$g_{B\_}(t_2)$: The j-th degree simulation result of B component at time t_2 on R.G.B domain
$SSI(t_2,j)$: The j-th degree scene simulation Image at time t_2　　t_1 :The time of the input image was taken

Fig. 6 The flow chart of the simulation image synthesis of a time scene.

3. Experiment results

Several test images with size (720 × 512) were used in simulation for demonstrating the performance of the proposed scheme. In order to give a detailed description of the simulation results, a series images and corresponding error tables are used to express the simulation results. Comparing the corresponding simulation images with the real images, we found more of the sky is dominated by pasted reds (or color orange), especially around the Sun. The shadow region is expanding and growing to more dark as the Sun goes down. The simulation images are almost the same as the real image except the cloud shape and the color at cloud's boundary. Table 5 shows the absolute error ratios of simulation image with respect

to the real image of Fig.7. From the error tables, one shall find that the error in B plane is the largest and the error in R plane is the smallest, this is caused by the fact that the average pixel value in R plane is larger than the average pixel value in B plane. On the other hand, the error in order 2 and order 3 best fitting regressions are much larger than the error in order 5 and order 6 best fitting regressions. This coincides with the Rayleigh scattering theory of sunlight. Experimental results show that there is no difference in human's visual sense between the simulation image obtained by our algorithm and the real image. However, because our algorithm is carried out in the DCT domain and use look-up table algorithm, it becomes time-saving and simpler.

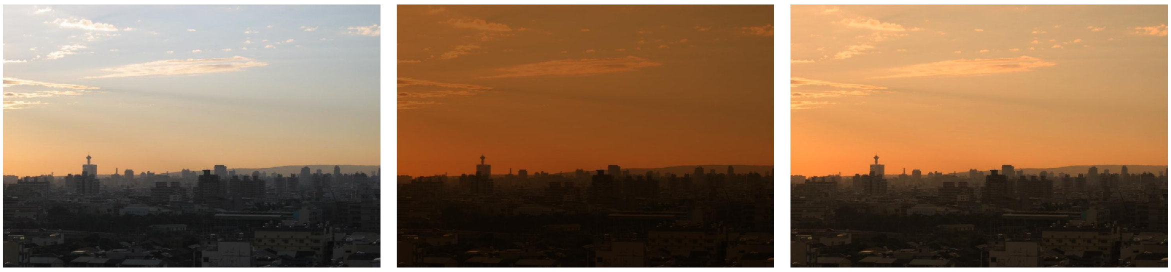

(a) (b) (c)

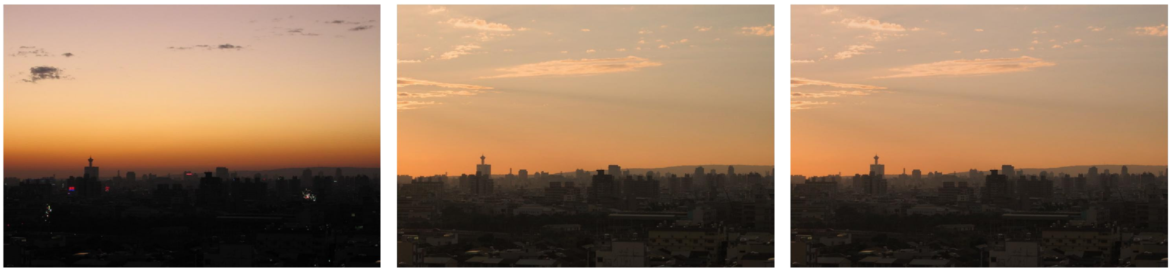

(d) (e) (f)

Fig.7.1 (a) the image of a scene photographed at 16:45 PM, (b) degree 2 simulation image at 17:30, (c) degree 3 simulation image at 17:30, (d) the image of the same scene photographed at 17:30 PM, (e) degree 5 simulation image at 17:30, (f) degree 6 simulation image at 17:30.

Table 5.1 Table of absolute error ratios of simulation image with respect to real image of Fig.7.1.

	Order2	Order3	Order4	Order5	Order6
Error in R plane(%)	37.4371	18.5745	20.3	18.5914	19.4012
Error in G plane(%)	51.551	19.502	20.41	19.2	20.2056
Error in B plane(%)	73.6245	28.5651	21.5646	20.9681	21.03
Complexity	n^2	n^3	n^4	n^5	n^6

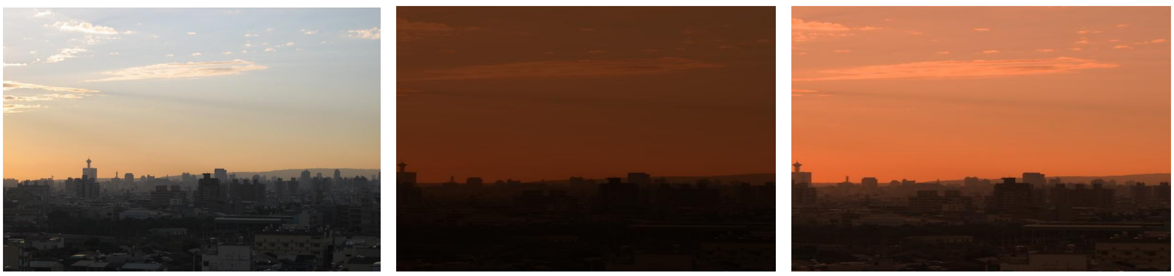

(a) (b) (c)

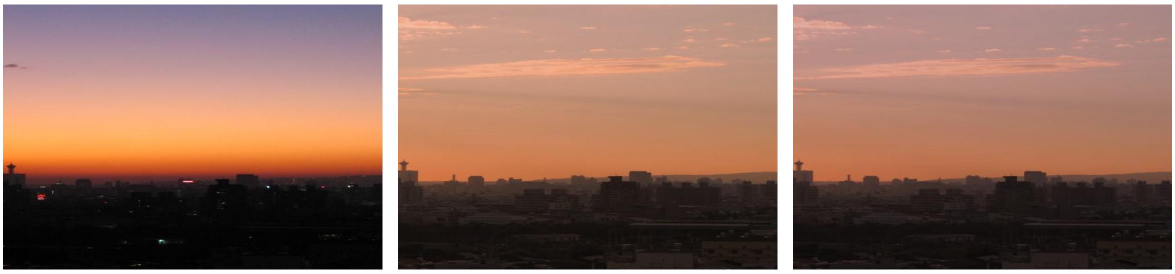

(d) (e) (f)

Fig.7.2 (a) the image of a scene photographed at 16:45 PM, (b) degree 2 simulation image at 17:40, (c) degree 3 simulation image at 17:40, (d) the image of the same scene photographed at 17:40 PM, (e) degree 5 simulation image at 17:40, (f) degree 6 simulation image at 17:40.

Table 5.2 Table of absolute error ratios of simulation image with respect to real image of Fig.7.2.

	Order2	Order3	Order4	Order5	Order6
Error in R plane(%)	54.2817	30.0294	28.174	28.4968	27.9642
Error in G plane(%)	67.222	25.2933	24.602	25.349	24.5042
Error in B plane(%)	82.4793	40.1093	26.9088	22.1554	22.1407
Complexity	n^2	n^3	n^4	n^5	n^6

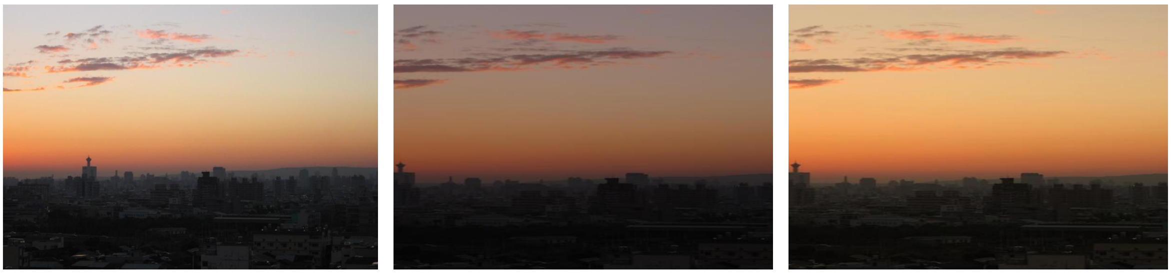

(a) (b) (c)

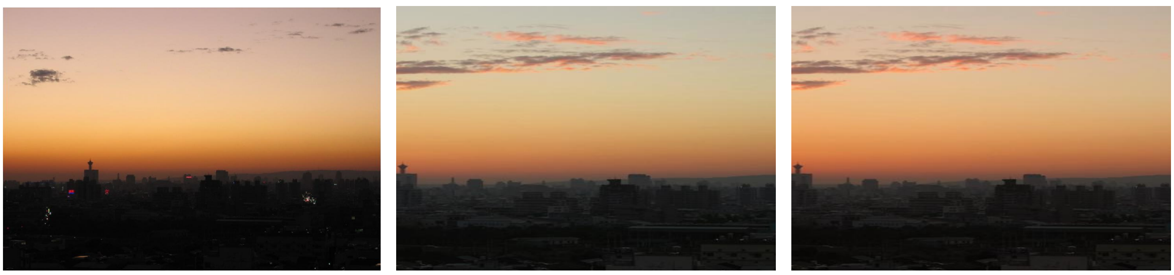

(d) (e) (f)

Fig.7.3 (a) the image of a scene photographed at 17:15 PM, (b) degree 2 simulation image at 17:30, (c) degree 3 simulation image at 17:30, (d) the image of the same scene photographed at 17:30 PM, (e) degree 5 simulation image at 17:30, (f) degree 6 simulation image at 17:30.

Table 5.3 Table of absolute error ratios of simulation image with respect to real image of Fig.7.3.

	Order2	Order3	Order4	Order5	Order6
Error in R plane(%)	33.3016	7.868	10.4042	10.5143	8.1667
Error in G plane(%)	35.335	12.03	11.8135	11.5513	11.8
Error in B plane(%)	30.1	19.706	14.019	13.8382	13.8
Complexity	n^2	n^3	n^4	n^5	n^6

(a) (b) (c)

(d) (e) (f)

Fig.7.4 (a) the image of a scene photographed at 17:15 PM, (b) degree 2 simulation image at 17:40, (c) degree 3 simulation image at 17:40, (d) the image of the same scene photographed at 17:40 PM, (e) degree 5 simulation image at 17:40, (f) degree 6 simulation image at 17:40.

Table 5.4 Table of absolute error ratios of simulation image with respect to real image of Fig.7.4.

	Order2	Order3	Order4	Order5	Order6
Error in R plane(%)	52.515	22.74	22.27	22.2144	22.2455
Error in G plane(%)	56.5317	22.0115	21.3354	22.3	20.89
Error in B plane(%)	53	33.8	16.6808	16.2357	16.444
Complexity	n^2	n^3	n^4	n^5	n^6

4. Conclusion

For any degree of best fitting simulation using a computer with Intel Pentium D 2.8GHz CPU and 512MB RAM, it only takes 3 seconds to simulate a scene image of size 720 × 512 by our look-up table algorithm. On the other hand, simulating the same image by regression simulation with the same computer takes more than 540 seconds. Table 5.1~Table5.4 are the tables of absolute error ratios of simulation with respect to real images. They show that the absolute error ratio of simulations approaches to a stable value less than 27% when the orders of regressions are larger than 4; this error in images almost can not be found by human eyes and it can be reduced by adopting more bands in DCT domain of images in the regression step. However, adopting more bands for regression is going to take more time and need more computer memory. With the above experimental results and performance analyses, we conclude that the proposed approach has three major advantages: (A) The reference database created from the time- series color-block images instead of using the scene images of a place is suitable for any outdoor scene taken at anywhere at anytime. (B) Taking the piecewise multiple regression on the DCT coefficients of scene images instead of taking the multiple regression on the spatial pixels of scene images, this approach simplifies the regression procedure and saves the processing time. (C) Using look-up table algorithm to save much simulation time. With this algorithm, one can successfully and effectively simulate the duck scene from an outdoor scene taken in the afternoon whether it is of uniform color or complex colors.

References

[1] Van de Hulst HC., "Light Scattering by small particles," Dover Publications, New York, 1981

[2] Maarten Sneep and Wim Ubachs, "Direct measurement of the Rayleigh scattering cross section in various gases," Journal of Quantitative Spectroscopy & Radiative Transfer, Vol. 92, pp. 293- 310, 2005.

[3] R. V. Deelen, J. Landgraf and I. Aben, "Multiple elastic light scattering in the Earth's atmosphere: a doubling- adding method to include rotational Raman scattering by air," Journal of Quantitative Spectroscopy & Radiative Transfer, Vol. 95, pp. 309- 330, 2005.

[4] S. M. Lea and J. R. Burke, "Physics: The nature of things", annotated instructor's edition 1997, West company, USA, pp. 597-626.

[5] W. B. Thompson, P. Shirley, and J. A. Ferwer, "A Spatial Post- Processing Algorithm for Images of Night Scenes," Journal of Graphics Tools, Vol. 7, No. 1, pp. 1- 12, 2003.

[6] T. Welsh, M. Ashikhmin, K. Mueller, Transferring color to greyscale images. Proceedings of 29th annual conference on computer graphics and interactive techniques, ACM Press, New York, USA, 2002, pp. 277–280.

[7] Alexander Toet ,'Colorizing single band intensified nightvision images', Displays, Vol. 26, No. 1, pp: 15-21, 2005

[8] Arthur R. Weeks, Jr., "Funamentals of Elecroni Image Processng", SPIE/IEEE Series on Image Science & Engineering, Bellingham, Washington USA, pp. 440-451, 1998.

[9] Angus M. Brown, "A step-by-step guide to non-linear regression analysis of experimental data using a Microsoft Excel spread sheet", Computer methods and programs in Biomedicine 65, pp. 191-200, 2001.

[10] C. J. Vianna, E. A. De Souza, Combining Marr and Canny Operators to Detect Edges, Microwave and Optoelectronics Conference, 2003. Vol. 2, pp. 695-699.

[11] E. Bourennane, P. Gouton, M. Paindavoine, F. Truchetet, Generalization of Canny- Deriche filter for detection of noisy exponential edge, Signal processing 82 (2002) 1317-1328.

[12] G. Qiu and J. Duan, "An Optimal Tone Reproduction Curve Operator for the Display of High Dynamic Range Images," IEEE International Symposium on Circuits and Systems, pp.6276-6279, 2005.

[13] G. W. Larson, H. Rushmeier, and C. Piatko, "A Visibility Matching Tone Reproduction Operator for High

Dynamic Range Scenes, "IEEE Trans. On Visualization and Computer Graphics, Vol. 3, No. 4, pp.291-236, 1997.
[14] H. Zhang and L. Lucchese, "A Fast Tone Reproduction Algorithm for High Dynamic Range Image Display," 2004 IEEE 6th Workshop on Multimedia Signal processing, pp. 275-278. 2004.
[15] J. A. Ferwerda, "Elements of Early Vision for Computer Graphics," IEEE Computer Graphics and Applications, Vol. 21, No.5, pp. 22-33, 2001.
[16] J. Tumblin and H. Rushmeler, "Tone Reproduction for Realistic Images, IEEE Computer Graphics and Applications, Vol. 13, No.6, pp. 42-48, 1993.
[17] M. Boutell and J. Luo, "Sunset Scene Classification Using Simulated Image Recomposition," Proceeding, IEEE Int'l Conf. on Multimedia and Expo, pp.I.37-I.40, 2003.
[18] M. Hermon, "Generating Detailed Scene Descriptions, "IEEE Int'l Conf. On Robotics and Automation, Vol. 2, pp.426-431, 1986.
[19] R. C. Gonzalez and R. E. Woods, "Digital image processing," 2nd ed., New Jersey: Prentice-Hall, 2002, pp. 675-683.
[20] C. C. Liu and W. Y. Chen, " Screw pitch pression measurement using simple linear regression and image analysis", Applied Mathematics and Computation, Vol. 178, pp.390- 404, 2006.
[21] J. S. Milton, J. C. Arnold, "Introduction to probability and statistics",4th edition 2003, McGraw-Hill companies, New York, pp. 448-457
[22] S.I.V. Sousa, F.G. Martins, M.C.M. Alvim-Ferraz, M.C. Pereira, "Multiple linear regression and artificial neural networks based on principal components to predict ozone concentrations", Environmental Modelling and Software, Vol. 22, No. 1, pp. 97-103, 2007
[23] Daidi Zhong , Irek Defée, "DCT histogram optimization for image database retrieval", Pattern Recognition Letters, Vol. 26, No. 14, pp. 2272-2281, 2005
[24] J. Tang, " A contrast based image fusion technique in the DCT domain", Digital Signal Processing, Vol. 14,p.218-226, 2004
[25] S. S. Deeb, "Genetics of variation in human color vision and the retinal cone mosaic", Current Opinion in Genetics & Development, Vol: 16 ,No.3, pp. 301-307, 2006
[26] Lennie, Peter, "Color vision: Putting it together", Current Biology, Vol. 10, No.16, pp. R589-R591, 2000
[27] S. D.Buluswar, B. A. Draper, "Color Models for Outdoor Machine Vision," Computer Vision and Image Understanding, Vol.85, No.2, pp. 71-99 , 2002
[28] C. Clausen and H. Wechsler, "Color Image Compression Using PCA and Backpropagation Learning, " pattern recognition, Vol. 33, pp1555-1560, 2000
[29] T. Bose, "Digital signal and image processing", 2004, J. Wiley & sons,New York
[30] I. Andreadis and Ph. Tsalides, "Analog computation of Image Chromaticity," Real-Time Imaging 3,pp.1-6, 1997
[31] J. S. Milton and J. C. Arnold, "Introduction to probability and statistics", 4th edition 2003, the McGraw-Hill companies, New York, pp.448-457
[32] C. Y. Huang and G. H. Tzeng, "Multiple generation product life cycle predictions using a novel two-stage fuzzy piecewise regression analysis method", Technological Forecasting & Social Change Vol.75, No.1, January, 2008, pp. 12-31